

Visual inspection via a global-to-local optimization method for agarwood sticks

An Yuan

Guangdong University of Technology

Nian Cai (✉ cainian@gdut.edu.cn)

Guangdong University of Technology

Zhouyixiao Wu

Guangdong University of Technology

Zhiliang Wu

Guangdong University of Technology

Shaoqiu Xu

Guangdong University of Technology

Weicheng Ou

Guangdong University of Technology

Han Wan

Guangdong University of Technology

Research Article

Keywords: visual inspection for agarwood, machine vision, global-to-local optimization, dissimilarity function, ash shrinkage rate, carbon line height

Posted Date: October 13th, 2022

DOI: <https://doi.org/10.21203/rs.3.rs-2146550/v1>

License:  This work is licensed under a Creative Commons Attribution 4.0 International License.

[Read Full License](#)

Visual inspection via a global-to-local optimization method for agarwood sticks

An Yuan¹, Nian Cai^{1,2*}, (✉), Zhouyixiao Wu¹, Zhiliang Wu¹, Shaoqiu Xu¹, Weicheng Ou², Han Wang²

Abstract

Chemical composition analysis, chromatography and spectroscopy are dominate quality evaluation methods for agarwood, which are cumbersome and time-consuming. To facilitate its quality evaluation, a global-to-local optimization method is proposed to automatically inspect the appearance of the burned agarwood stick. First, a dissimilarity coefficient is defined by the attributes of the connected domains to coarsely localize the carbon line region. Then, the threshold for the coarsely localized carbon line region is adaptively determined based on grayscale characteristics of image patches partitioned from the coarsely localized carbon line region. Next, the threshold is used to extract the contour of the carbon line region and to establish the fine localization model for locally and precisely localizing the carbon line region. Finally, an ash shrinkage compensation coefficient is defined to calculate the ash shrinkage rate (ASR). The ASR combined with carbon line height is utilized to characterize the appearance of burned agarwood. Experimental results indicate that the proposed inspection method can well detect the carbon line regions and ashes of burned agarwood sticks, with a mean ASR error of 0.74%, which is superior to some existing inspection methods.

Keywords visual inspection for agarwood, machine vision, global-to-local optimization, dissimilarity function, ash shrinkage rate, carbon line height

1 Introduction

Agarwood is a fragrant wood of Thymelaeaceae which has been used as a valuable incense for ages. With the maturity of production technology, incense sticks are widely used as the main incense carrier [1]. In addition, incense therapy is a common therapy in the field of traditional Chinese medicine, such as for allergic rhinitis [2], and herpes zoster [3]. Also, agarwood is widely used in cosmetology and religion. However, due to the excellent quality and the scarcity of wild Agarwood [4], counterfeit and inferior agarwood products are circulating in the market [5]. Therefore, quality evaluation of Agarwood is practically significant.

Agarwood contains unique effective active ingredients, such as 2-(2-phenylethyl)chromone, 6,7-dimethoxy-2-(2-phenylethyl)chromone, 6,7-dimethoxy-2-[2-(4'-methoxyphenyl)ethyl]chromone and sedum tetrol. The contents of these ingredients are crucial to the quality evaluation of agarwood. Current quality evaluation methods mainly include chemical composition analysis, chromatography and spectrometry [5-7]. However, these methods are time-consuming and cumbersome for operation. Specifically, For spectrometry [8], the spectral cube of the agarwood is achieved to extract its spectral features, which are used to establish a standard database of agarwood. Then, the spectral cube of the inspected agarwood product is compared with the standard database of agarwood to evaluate its quality. Spectrometry requires bulky and expensive hardware, and its manual operation is cumbersome.

The category and content of organic chemical ingredients contained in a substance affect its burning speed and consequently affect its appearance during burning [9-10]. For example, cigarettes containing different organic substances such as ketones and alcohols have different burning speeds, resulting in differences in appearance during burning. Thus, some studies [11-13] utilized these appearance diversities to manually evaluate qualities of the cigarettes, in which the ash and carbon line is manually and offline labelled for the acquired burned cigarette image. Although this manual evaluation utilizes machine vision to evaluate the quality of the substance by the burning metrics such as ash shrinkage rate (ASR) and carbon line height, its offline operation cannot automatically calculate these metrics during burning, which also brings a lot of operation burden for the quality control (QC) worker. In any case, these studies provide a machine vision strategy to evaluate the quality of some substance via the burning metrics due to its burning characteristics, which inspires us to propose an automatic machine vision method to online evaluate the quality of agarwood.

However, the appearance of the burned agarwood stick constantly changes over time, which results in the constant changes of the carbon line and the ash. In practice, the carbon line is a region rather than a line, in which gray values of pixels gradually change to make the burning boundary indistinct. Moreover, different categories of agarwood have different burning characteristics, which results that the appearances of the burned agarwood stick of different categories are quite different even if they are burned under the same burning condition. These facts aggravate the challenge of automatic visual inspection of agarwood sticks during burning.

To automatically and online inspect the burned agarwood sticks, a machine vision strategy is proposed in this paper, which involves a designed image acquisition system and a global-to-local optimization scheme. First, the target dissimilarity function [14-16] is introduced to define a dissimilarity coefficient by means of the attributes of the connected domains extracted from the agarwood

✉ Nian Cai
cainian@gdut.edu.cn

1. School of Information Engineering, Guangdong University of Technology, Guangzhou, 510006, China
2. State Key Laboratory of Precision Electronic Manufacturing Technology and Equipment, Guangdong University of Technology, Guangzhou 510006, P.R. China

stick image, which is utilized to coarsely localize the carbon line. Then, the threshold is adaptively determined based on the grayscale characteristics of image patches of the coarsely localized carbon line region, which is utilized for extracting the contour of the carbon line region. Next, a fine localization model is established to locally and precisely localize the carbon line region. Finally, an ash shrinkage compensation coefficients is defined to deal with the inspection errors caused by the changes in terms of the scene and the category of the agarwood stick. Thus, two important metrics of ASR and carbon line height can be calculated to characterize the appearance of burned agarwood stick.

The contributions of our work can be summarized as followings.

(1) A machine vision system is established to automatically and online inspect the appearances of burned agarwood sticks, which involves a designed image acquisition system and a global-to-local optimization method.

(2) A dissimilarity coefficient is defined to formulate the global optimization scheme to coarsely localize the carbon line region, which involves the attributes of the connected domains extracted from the burned agarwood stick image.

(3) To cope with different categories of agarwood sticks and scene illumination changes, a local optimization scheme is proposed based on the adaptive grayscale threshold for the carbon line region, which can locally and precisely localize the carbon line region. The ash shrinkage compensation coefficient is defined by integrating the dissimilarity coefficient and the locally localized carbon line region, which can be utilized to achieve the metric of ASR.

2. Image acquisition

An image acquisition system is designed for the visual inspection of agarwood sticks, as shown in Fig. 1. It consists of two white LED strip light sources, a Basler CCD industrial camera with the resolution of 1388×1038 pixels, a circular rotating stage, and a blue background board. It is noted that 10 agarwood sticks can be online inspected in one experiment. The rotating stage is automatically rotatee every 6 seconds to deliver an agarwood stick into the view of the industrial camera. The acquired images via the camera are transmitted to the industrial computer for inspection, which is implemented by the designed machine vision software involving the proposed global-to-local optimization method.

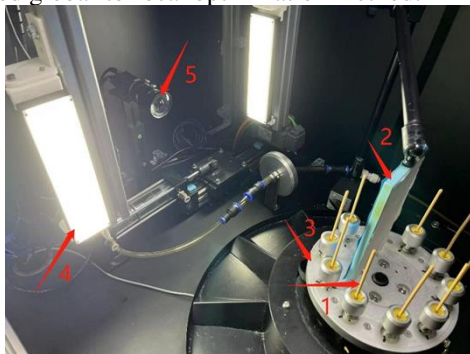


Fig 1 Image acquisition system for agarwood sticks 1. agarwood stick. 2. background board. 3. Rotating stage. 4. White LED strip light sources. 5. Industrial CCD camera.

In this study, three different categories of agarwood sticks are employed to validate our proposed inspection system. For each category, 500 images of the burned agarwood stick at different burning moments are acquired by the designed image acquisition system. Fig. 2 illustrates an example of the burned agarwood stick. As shown in Fig. 2, the ash region and the carbon line region demonstrate gray and black, respectively. However, it is noted that a crack emerging in the ash region also demonstrates black, which results in possible mis-detection for carbon line region.

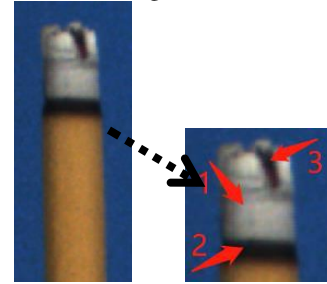


Fig 2 An example of the burned agarwood stick. 1. Ash region; 2. Carbon line region; 3. Crack.

As indicated in Fig. 3, the appearance of the carbon line region changes over time during the burning of the agarwood stick, which results in the appearance change of the ash region. In real industries, thresholding is a promising and commonly-used method to detect the regions of interest (ROIs)[17-19], in which appropriate threshold is significant. In this paper, the threshold for extracting the contour of the carbon line region is adaptively determined based on image patches partitioned from the coarsely localized carbon line region, which will be described in Section 3.3.



Fig. 3 Some examples of carbon line regions of burned agarwood sticks.

3 The proposed inspection method

3.1 Architecture of the inspection method

Fig. 4 illustrates the architecture of the proposed inspection method, which in order involves ROI extraction, global optimization for coarse localization, local optimization for fine localization and metrics calculation. Since the agarwood stick is fixed on the rotating stage and delivered to the view of the camera by the rotating stage, the agarwood stick localizes in the center view of the acquired image. Thus, the ROI of the agarwood stick can be simply extracted by a fixed window from the acquired image by the image acquisition system. In the stage of global optimization, the attribute vectors are first constructed for connected domains detected from the ROI, which can characterize the connected domains in terms of their profiles. Then, the dissimilarity coefficient is defined by the attribute vectors, which is utilized to establish the global optimization model for coarse localization of the carbon line region. In the stage of local optimization, the threshold for the carbon line region is adaptively

determined for each burned agarwood stick at any moment, which is utilized to establish the local optimization model for fine localization of the carbon line region. Finally, the carbon line height can be calculated by the finely localized carbon line region. To calculate the ASR, a compensation coefficient is defined by integrating the dissimilarity coefficient, the morphological parameters of the contour and the bounding box of the carbon line region.

3.2 Global optimization for coarse localization of carbon line region

As discussed in Section 2, both of the crack and the carbon line region demonstrate black. Especially, the transverse crack has the similar profile to the carbon line region, except for their sizes. The facts will result that the transverse crack is possibly inspected as the carbon line region. To deal with this problem, a dissimilarity coefficient is defined to evaluate the difference between the crack and the carbon line region, formulated as

$$D_{E\tau}(x_\tau, r_\tau) = \|x_\tau - r_\tau\| = \sqrt{(x_\tau - r_\tau)^T(x_\tau - r_\tau)} \quad (1)$$

$$x_\tau = \begin{pmatrix} \beta_1 d^2 \\ \beta_2 A_\tau \\ \beta_3 S_\tau \end{pmatrix}, \quad \tau = 1, 2, \dots, n \quad (2)$$

$$r_\tau = \begin{pmatrix} \beta_1 d_{\tau\lambda}^2 \\ \beta_2 S_{\tau\lambda} \\ \beta_3 S_{\tau\lambda} \end{pmatrix}, \quad \tau = 1, 2, \dots, n \quad (3)$$

where r_τ and x_τ are the attribute vectors of the potential crack and the potential carbon line region, respectively, both of which are the connected domains in the ROI of the acquired image. d is the diameter of the agarwood stick. A_τ and S_τ are the areas of the potential carbon line region and its bounding box, respectively. $d_{\tau\lambda}$ and $S_{\tau\lambda}$ are the width and the area of the bounding box of the potential crack, respectively. β_1 , β_2 , and β_3 are three attribute coefficients satisfying

$$\beta_1 + \beta_2 + \beta_3 = 1 \quad (4)$$

$$\begin{cases} \beta_1 \geq 0.1 \\ \beta_2 \geq 0.1 \\ \beta_3 \geq 0.1 \end{cases} \quad (5)$$

It is noted that (5) is to ensure that each attribute coefficient contributes to the dissimilarity coefficient. In this paper, they are empirically set as $\beta_1=0.8$ and $\beta_2=\beta_3=0.1$, which will be experimentally verified in Section 4.1.

The connected domain with minimal dissimilarity coefficient is inspected as the potential carbon line region, formulated as

$$D_E = \min \{D_{E\tau}(x_\tau, r_\tau)\} \quad (6)$$

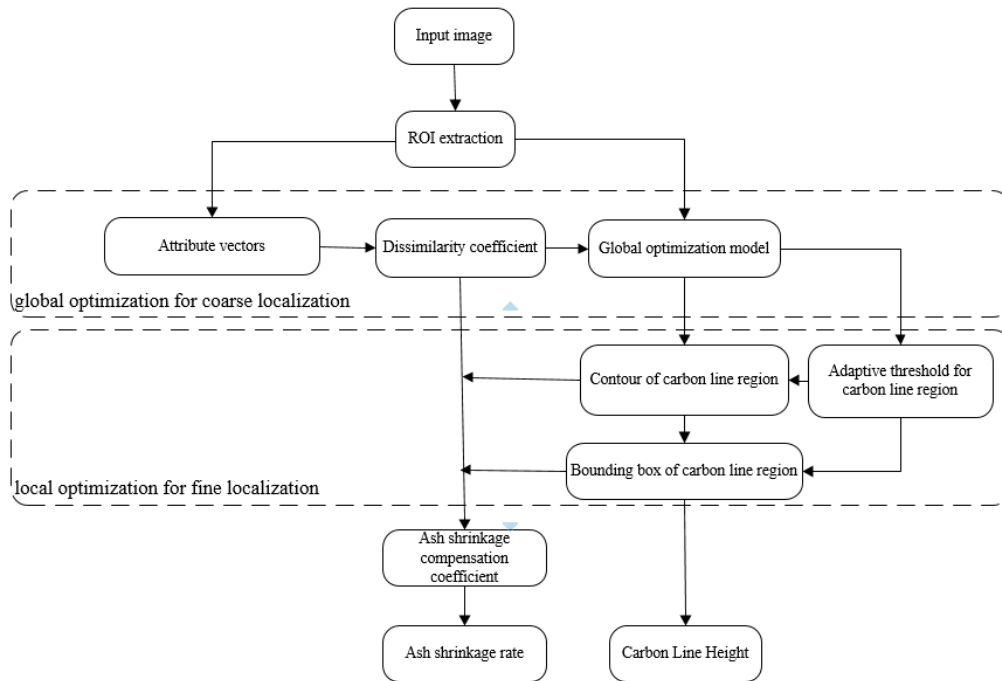


Fig. 4 The architecture of the proposed inspection method.

3.3 Local optimization for fine localization

Different categories of agarwood sticks have different burning characteristics, which results in different grayscale changes in the carbon line region. Moreover, the ash inevitably warps during burning, resulting in burrs on the edge of the carbon line region. These burrs will result that the global optimization cannot precisely localize the carbon line region. To suppress the influence of burrs, a global optimization scheme is proposed to finely localize the carbon line based on the coarse localization, which is described as follows.

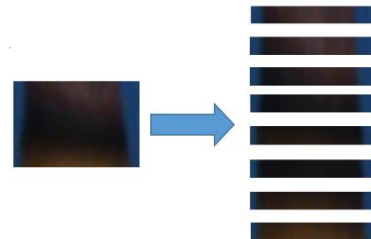


Fig. 5 Image patches partitioned by the coarsely localized carbon line region.

First, the coarsely localized carbon line region is vertically partitioned into k image patches, as shown in Fig. 5. The average gray value of each image patch is calculated and then top-to-bottom arranged as

$$\{Y(1), \dots, Y(i), \dots, Y(k)\} \quad (7)$$

The threshold ϖ for the carbon line region is adaptively determined as

$$\varpi = \max |Y(i+1) - Y(i)| + Y(i) \quad (8)$$

Then, the contour of the carbon line region can be extracted by means of the adaptive threshold, which can be utilized to determine the bottom and top of the bounding box of the carbon line region. Due to burrs emerging on the contour of the carbon line region, the bounding box does not envelop the carbon line region tightly in height direction, which will result in the inspection precision in terms of carbon line height and ASR. Since the width of the carbon line region can be determined in the stage of global optimization, local optimization is to determine the appropriate bottom and top of the bounding box (l_1, h_1) , which are formulated as

$$(l_1, h_1) = \{(l_1, h_1) | \min |(\Phi(\varepsilon, l) - \gamma\varpi), \min |(\Phi(\varepsilon, h) - \gamma\varpi)\} \quad (9)$$

s.t. $l_0 \leq l \leq h_0, l_0 \leq h \leq h_0$

where (l_0, h_0) is the bottom and top positions of the bounding box of the coarsely localized carbon line region in height direction. $\Phi(\varepsilon, l)$ and $\Phi(\varepsilon, h)$ denote the average grayscale values of the block between l and $l+\varepsilon$ and the block between h and $h-\varepsilon$, respectively. γ is the adjustment factor, which is set to 1.5 empirically. ε is the searching step, which changes in the stage of local optimization for the trade-off of speed and precision.

3.4 Metrics for inspection of agarwood sticks

In this paper, carbon line height and ASR are used as the metrics for visual inspection of burned agarwood sticks.

Carbon line height (CLH) is defined as the height of the bounding box of the carbon line region finely localized by the local optimization scheme, formulated as

$$CLH = h_1 - l_1 \quad (10)$$

ASR is defined as

$$ASR = \frac{s - (s_1 + p)}{s} \times 100\% \quad (11)$$

where S_l and S are the areas of ash and its bounding box (shown in Fig. 6), respectively. p is the ASR compensation coefficient, defined as

$$p = \frac{D_E^t}{\max(D_E^t)_{t \in [0, t]}} (A_1 - A_2) \quad (12)$$

where D_E^t is the dissimilarity coefficient at the t moment, A_2 and A_1 are the areas of the carbon line region and its bounding box.

As indicated in (10-12), the smaller the height of the CLH and the greater the ASR, the better the quality of the agarwood stick.

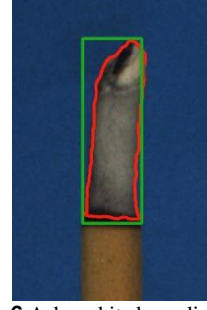


Fig. 6 Ash and its bounding box

4. Experimental results and discussions

4.1 Influence of attribute coefficients

As described in Section 3.2, three attribute coefficients influence the constructions of the attribute vectors of the connected domains in the ROI of the acquired agarwood stick image, which further influence global optimization for coarse localization. In this section, we have conducted an experiment to discuss their influences on global optimization, in which they follow the constraints in (4-5).

As indicated in Fig. 7, the dissimilarity coefficient increases with the increase of β_1 and the decrease of β_2 simultaneously. As discussed in Section 2, the smaller the dissimilarity coefficient, the higher the probability that a crack is inspected as a carbon line region, which will result in mis-inspection. And vice versa. Thus, in this paper, three attribute coefficients are experimentally set as $\beta_1=0.8$ and $\beta_2=\beta_3=0.1$, as indicated in Fig. 7.

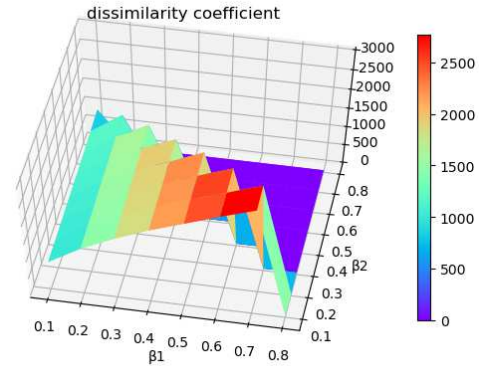


Fig. 7 Influence of attribute coefficients on global optimization.

Table 1 Calculated carbon line heights for different adjustment factors.

γ		1.2	1.3	1.4	1.5	1.6	1.7	1.8
CLH (pixels)	40 (ground truth)	31(± 7)	33(± 5)	35(± 5)	42(± 3)	46(± 5)	54(± 5)	60(± 7)

4.2 Influence of adjustment factor γ

As indicated in (9), the adjustment factor γ influences the performance of global optimization for fine localization of the carbon line region. We have conducted an experiment to discuss the influence of adjustment factor on local optimization, in which the carbon line heights (CLHs) are

calculated by (9) with different adjustment factors. It is noted that the ground-truth CLH is 40-pixels.

As indicated in Table 1, the calculated CLH increases with the increase of γ . The calculated CLH approaches the ground truth when $\gamma=1.5$. So, the adjustment factor is empirically set to 1.5 in this paper.

4.3 Comparisons of other methods

Although no automatic inspection methods have been employed for agarwood sticks, we have compared our method with three existing target detection methods since target detection is a key step in this inspection task, which are DSCD [20], YOLOv4 [21], and CCHS [22]. For fair comparisons, DSCD, CCHS and our method are used for image segmentation (Fig. 8) to achieve the contours of carbon line region (Fig. 9), all of which are followed by our local optimization scheme to precisely calculate carbon line heights. Since the carbon line region can be directly detected by means of a bounding box by YOLOv4, the contour of carbon line region can be easily achieved from the bounding box. Similarly, the ashes and their bounding boxes can be also detected. All the ground truths are obtained by manually sketching the carbon line region via the Labelme software.

As illustrated in Figs. 8-10, the carbon line regions and their contours detected by the DSCD and the CCHS are larger than their ground-truths, which results in their bounding boxes do not tightly envelop the carbon line regions. This is possibly because the DSCD is an edge

mapping method and the CCHS is a contour searching method, both of which are highly dependent on the grayscale differences between the target and its surroundings. However, burned agarwood sticks show no significant boundaries in terms of grayscale between the carbon line region and its surroundings, which will limit the applications of DSCD and the CCHS for the agarwood stick inspection. YOLOv4 is a data-driven detection method, which requires high-quality annotation to train the network. However, there is no salient boundary between the carbon line region and its surroundings, which will result in two problems. One is that the annotation is highly subjective and the other is that burrs influence the detection. Thus, the two problems result that there are relatively salient differences between the detected results via YOLOv4 and the ground truths. Our proposed inspection method extracts the carbon line regions and the carbon line contours from the acquired images, which are highly similar to the ground truths. Consequently, their bounding boxes tightly envelop the carbon line regions, which are almost the same as the ground truths. This can be contributed to the two schemes in the proposed inspection method. One is global optimization involving dissimilarity coefficient with attribute vectors, which can well suppress the interference of cracks to coarsely localize the carbon line region. The other is local optimization involving patch-based adaptive thresholding, which can well suppress the interference of burrs to finely localize the carbon line region.

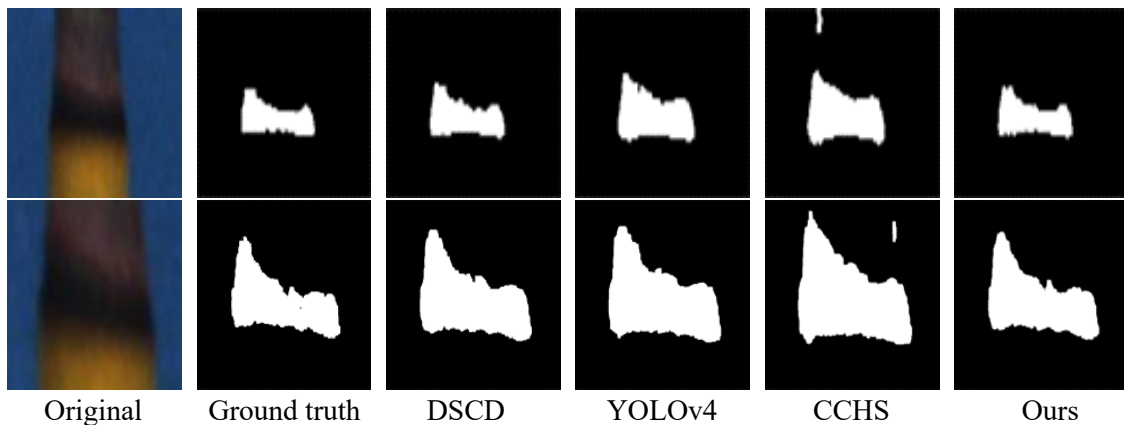


Fig. 8 Segmentation of carbon line regions.

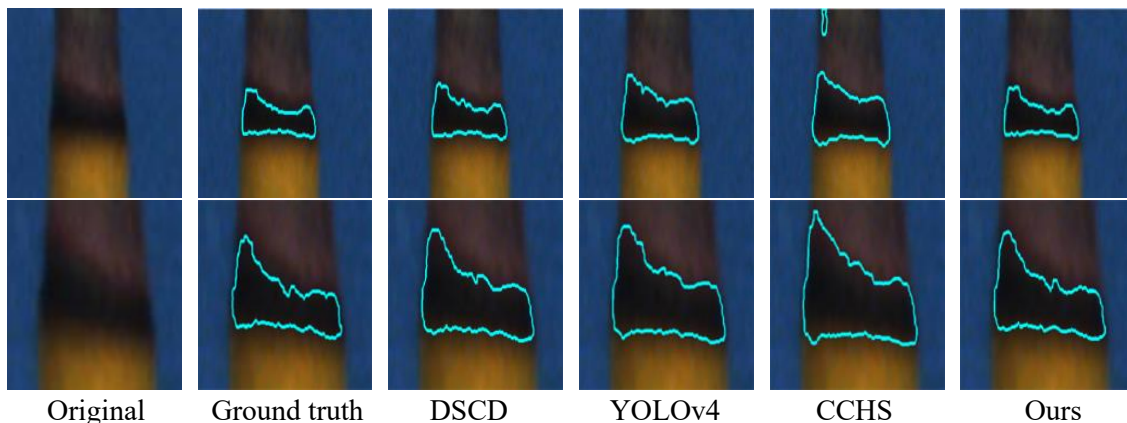


Fig. 9 Contour extraction of carbon line regions.

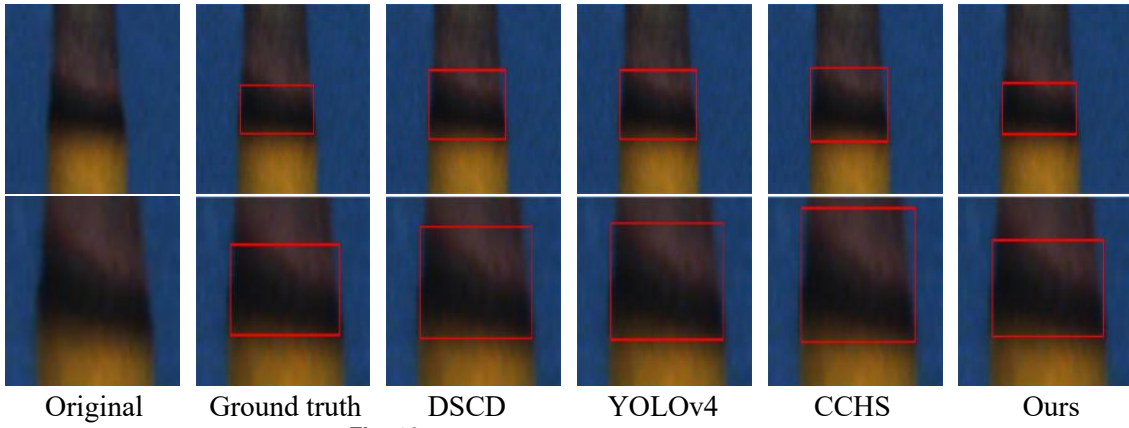


Fig. 10 Bounding boxes for carbon line regions.

Table 2 CLHs calculated by different methods with respect to different ash heights (pixel)

Methods	Ash height (pixels)						mCLH (pixels)
	50 (± 10)	70 (± 10)	90 (± 10)	110 (± 10)	70 (± 10)	50 (± 10)	
groundtruth	40	37	38	38	40	38	38.50
DSCD	44	43	44	44	45	43	43.83
YOLOv4	43	44	45	45	44	43	44.00
CCHS	46	45	47	43	46	44	45.17
Ours	38	40	39	41	44	40	40.33

To further validate our proposed inspection method, carbon line heights (CLH) and ash shrinkage rate (ASR) are calculated for the burned agarwood sticks at different moments. For simple and intuitive explanations, we use different ash heights to indicate different moments for burned agarwood sticks. Also, mean CLH (mCLH) and mean ASR error are employed to evaluate the overall inspection during burning. Mean ASR error is defined as the mean of the deviations between the calculated ASRs and their ground truths at different burning moments.

As indicated in Tables 2-3, the CLHs and ASRs calculated by all the inspection methods deviate from the ground truths to different extents. Specifically, mCLH and

mean ASR calculated by the existing methods are all more than 5 pixels and more than 2%, respectively. Comparatively, our inspection method achieves better metrics of CLH and ASR than the three existing methods, with the mCLH of 40.33 pixels and mean ASR error of 0.74%. In particular, our proposed method with the ASR compensation coefficient calculates the ASR more precisely than that without the ASR compensation coefficient, with mean ASR errors of 0.74% vs. 1.70%, which demonstrates the effectiveness of the ASR compensation coefficient. These quantitative results are consistent with the previous visual analysis.

Table 3 ASRs calculated by different methods with respect to different ash heights (%)

Method	Ash height (pixels)						Error (%)
	50 (± 10)	70 (± 10)	90 (± 10)	110 (± 10)	130 (± 10)	150 (± 10)	
groundtruth	24.74	25.12	24.65	25.68	25.31	25.02	
DSCD	27.30	27.63	27.21	28.16	27.98	27.74	2.57
YOLOv4	26.44	27.77	28.35	26.30	28.02	27.88	2.71
CCHS	26.56	27.88	28.46	27.41	28.13	28.99	2.82
Ours(without compensation)	25.44	26.76	27.34	26.29	27.01	27.87	1.70
Ours(with compensate)	25.48	25.86	25.39	26.42	26.05	25.76	0.74

5. Conclusions

The appearances of carbon line regions and ashes of burned agarwood sticks can be used to implicitly assess the qualities of agarwood sticks. In this paper, we propose a machine vision system to inspect the appearances of burned agarwood sticks, which involves a designed image acquisition system and a global-to-local optimization method for inspection. The proposed inspection method

consists of a global optimization scheme with the defined dissimilarity coefficient for coarsely localizing the carbon line region and a local optimization scheme with the proposed adaptive thresholding for finely localizing the carbon line region. For precisely calculating the ASR, a defined compensation coefficient is incorporated into the definition of the ASR.

Experimental results show that appropriate attribute coefficients and proper adjustment factor are beneficial to global optimization and local optimization, respectively, which influence the inspection performance of the proposed global-to-local method. Visual and statistical

experiments indicate that our proposed method can better inspect the appearances of agarwood sticks at different burning moments than several existing detection methods.

In this paper, two metrics of CLH and ASR are defined for evaluating the inspection of agarwood sticks, which can implicitly reveal the qualities of agarwood sticks. In the future, more metrics can be defined for this inspection task, such as the regularity of the carbon line region. This can be calculated by the longitudinal integrals of the finely localized carbon line region. Also, another issue can be studied in the future, in which several metrics are integrated to assess the qualities of agarwood sticks based on big data analysis of burned agarwood sticks.

Declarations

Competing interests

No potential conflict of interest was reported by the authors.

Authors' contributions

An Yuan and Nian Cai proposed ideas and methodologies, designed the experimental scheme and wrote the main manuscript text. Zhiliang Wu and Weicheng Ou assisted in the experiment and prepared figures. Shaoqi Xu, Zhouyixiao Wu and Han Wang reviewed and modified the manuscript.

Funding

No funding is received

Availability of data and materials

no data is available

References

1. Nor Azah Mohd Ali, Nurlaila Ismail, Mohd Nasir Taib, "Analysis of Agarwood Oil (*Aquilaria Malaccensis*) Based on GC-MS Data", 2012 IEEE 8th International Colloquium on Signal Processing and its Applications. DOI: <https://ieeexplore.ieee.org/document/6194771>
2. L.Y.Pan, X.M.Nong, S.M.Lu, "Clinical observation of thread-fragrance moxibustion in the treatment of acute episode allergic rhinitis[J]", *Chinese and Foreign Medical Research*, 2012, 10(34):41-42.
3. X.J.Han, R.R.Zhang, J.T.Liu, "19 Cases of herpes zoster treated by self-made traditional Chinese medicine thread-fragrance moxibustion combined with blood-letting puncture and cupping[J]. *China Naturopathy*", 2019, 27(13): 17-18.
4. Nurlaila Ismail, Mohd Hezri Fazalul Rahiman et al, "Investigation of Common Compounds in High Grade and Low Grade *Aquilaria Malaccensis* using Correlation Analysis", 2012 IEEE Control and System Graduate Research Colloquium (ICSGRC 2012). DOI: <https://ieeexplore.ieee.org/document/6287176>
5. Nurlaila Ismail, Mohd Hezri Fazalul Rahiman, Mohd Nasir Taib et al., "Identification of Significant Compounds of Agarwood Incense Smoke Different Qualities using Z-Score", 2015 IEEE 11th International Colloquium on Signal Processing & its Applications (CSPA2015), 6-8 Mac. 2015, Kuala Lumpur, Malaysia. DOI: <https://ieeexplore.ieee.org/document/7225646>
6. Nurlaila Ismail, Mohd Hezri Fazalul Rahiman, Mohd Nasir Taib, et al., "Observation on SPME Different Headspace Fiber Coupled with GC-MS in Extracting High Quality Agarwood Chipwood", 2016 IEEE International Conference on Automatic Control and Intelligent Systems (I2CACIS), 22 October 2016, Shah Alam, Malaysia. DOI: <https://ieeexplore.ieee.org/document/7885317>
7. Y.J.Fu, L.N.Tang, Y. Chen, et al, "Agarwood quality classification based on chemical composition analysis[J]", *China Forest Products Industry*, 2020, 57(10): 26-30, 64.
8. S.W.Huang, J.Zhao, T.Y.Liu, et al, "A method for non-destructive identification of the authenticity of Agarwood", Patents for inventions: CN201610003148.X.
9. Nurlaila Ismail, Mohd Hezri Fazalul Rahiman, Mohd et al, "A Review on Agarwood and Its Quality Determination", 2015 IEEE 6th Control and System Graduate Research Colloquium, Aug. 10-11, UiTM, Shah Alam, Malaysia. DOI: <https://ieeexplore.ieee.org/document/7412473>
10. Q.Zhao, Y.Wang, B.Zhang, "The Influence of Straw Shape on the Formation of Deposits during Straw Briquette Combustion", 2011 International Conference on Computer Distributed Control and Intelligent Environmental Monitoring. DOI: <https://ieeexplore.ieee.org/document/5748286>
11. F.Zheng, C.C.Xiao, S.Wang, Y.P.Zhang, Q.Z.Huang, L.Xiang, "The effect of cigarette paper characteristics on the static pack ash performance of cigarettes [J]", *Tobacco Science & Technology*, Mar.2020 Vol.53 No.3.
12. W.J.Chu, J.H.Cui, J.M.Wang, et al., "Cigarette static pack ash comprehensive evaluation method based on cigarette paper parameters [J]", *Tobacco Science & Technology*, Nov.2021 Vol.54 No.11.
13. S.Wang, L.Q.Xu, H.Dong, et al., "Cigarette burst bead trailing defect detection method [J]", *Tobacco Science & Technology*, 2021, 54(1):77-84.
14. X.D.Zhang, "Matrix Analysis and Applications" (2nd Edition), Tsinghua University Press, 2013.
15. L.Liu, Y.Zhang, M.Zhang, Y.Wang, J.Chen, "Analysis and optimization of ship trajectory dissimilarity models based on multi-feature fusion", *Journal of Traffic and Transportation Engineering*, Vol .21 No.5 Oct.2021. DOI: <http://transport.chd.edu.cn/article/doi/10.19818/j.cnki.1671-1637.2021.05.017>
16. Mikhail Usvyatsov, Konrad Schindler, "Visual recognition in the wild by sampling deep similarity functions", 2019 International Conference on Robotics and Automation (ICRA). DOI: <https://ieeexplore.ieee.org/document/8794162>
17. F.Xie, R.Chen, Q.Zhou, Y.Zhao, T.Sui, "An Adaptive Defect Detection Technology for Car-Bodies Surfaces", Year: 2019 | Conference Paper. DOI: <https://ieeexplore.ieee.org/document/8996176>
18. C.Wang, J.Yang, H.Lv, "Otsu Multi-Threshold Image Segmentation Algorithm Based on Improved Particle Swarm Optimization", 2019 2nd IEEE International Conference on Information Communication and Signal Processing. DOI: <https://ieeexplore.ieee.org/document/8958573>
19. C. Liu, F. Xie, Member, IEEE, X. Dong, H. Gao, and H. Zhang, "Small Target Detection From Infrared Remote Sensing Images Using Local Adaptive Thresholding", *IEEE JOURNAL OF SELECTED TOPICS IN APPLIED EARTH OBSERVATIONS AND REMOTE SENSING*, VOL. 15, 2022. DOI: <https://ieeexplore.ieee.org/document/9714810>
20. A. Manno-Kovacs, Member, IEEE, "Direction Selective Contour Detection for Salient Objects", *IEEE Transactions On Circuits And Systems For Video Technology*, VOL. 29, NO. 2, February 2019. DOI: <https://ieeexplore.ieee.org/document/8288650>
21. A. Bochkovskiy, C. Wang Institute of Information Science Academia Sinica, Taiwan, H. Liao Institute of Information Science Academia Sinica, Taiwan, "YOLOv4: Optimal Speed and Accuracy of Object Detection".
22. S. Wang, S. Yang, Senior Member, IEEE, M. Wang, and L. Jiao, Fellow, IEEE, "New Contour Cue-Based Hybrid Sparse Learning for Salient Object Detection", *IEEE Transactions On Cybernetics*, VOL. 51, NO. 8, AUGUST 2021. DOI: <https://ieeexplore.ieee.org/document/8945181>